

NATIONAL TRANSPORTATION SAFETY BOARD

Office of Research and Engineering
Vehicle Performance Division
Washington, D.C. 20594



April 30, 2015

FINITE ELEMENT MODELING STUDY REPORT

Final Version

A. ACCIDENT INFORMATION

Place : Manhattan, New York
Date : March 12, 2014
Operator : Consolidated Edison Company of New York, Incorporated (Con Edison)
Vehicle : Natural gas pipe
NTSB No. : DCA14MP002
Investigator : Ravi Chhatre, RPH-20

B. TOPICS ADDRESSED

Finite element modeling was used in an exploratory fashion to study various possible loading scenarios for the polyethylene pipe assembly. The study examined two zones of cracking in the pipe assembly. The first zone of cracking was in the saddle fusion between the main pipe and the tapping tee. The second zone of cracking was in the tapping tee body.

C. DETAILS OF THE STUDY

A 3D finite element model of the polyethylene pipe assembly was constructed in Abaqus 6.14-1 based on drawings and measurements. An initial area of separation was created at the saddle fusion joint based on the condition of the accident pipe assembly. The model was subjected to analyses of possible failure scenarios focusing on the tapping tee.

1. Geometry

a. Pipe assembly

The modeled pipe assembly consists of three components: the main pipe, the service pipe and the tapping tee/electrofusion coupling [Reference 1]. The main pipe has an 8.6-inch outside diameter (OD) and the service pipe has a 2.375-inch OD. In the model, the average measured values [Reference 1] of the diameter and wall thickness were used. The values for nominal and modeled dimensions for both pipes are shown in table 1.

Table 1. Measured and modeled dimensions of the pipes.

		Measured (inch)	Modeled (inch)
Main pipe	OD	8.6	8.6
	Wall thickness	0.822	0.822
Service pipe	OD	2.375	2.375
	Wall thickness	0.222	0.222

The geometry of the tapping tee was created based on a diagram supplied by George Fischer Central Plastics [Figure 5 of Reference 1] and measurements. The cap and the metal cutter were not modeled as neither was necessary for the purpose of this study. The threaded region of the tapping tee was not modeled for the same reason. The tapping tee was connected to the service pipe via an electrofusion coupling [Figures 1 through 3 of Reference 1], which was also included in the model. The geometry of the electrofusion coupling was created based on the product catalog [Reference 2] and measurements. The created tapping tee/electrofusion coupling model is shown in figure 1. The model of the pipe assembly is shown in figure 2. The modeled lengths of the main pipe and service pipe are 5 feet and 3 feet in figure 2 and different lengths were used in later models.

b. Main Pipe to saddle tee fusion zone

It was found [Reference 1] that the fracture between the pipe and the tapping tee intersected the fusion interface over an arc of approximately 210 degrees (labeled Regions 1 and 2 in Reference 1). In modeling, the part of the tapping tee saddle mating surface corresponding to Regions 1 and 2 was created as a separated region by partitioning the mating surface. Figure 3 shows the modeled area of separation, with comparison to the photograph of the actual saddle fusion fracture surface.

2. Material properties

All components of the pipe assembly were made from high density polyethylene (HDPE) material. Mechanical testing was performed on both the main pipe and tapping tee materials [Reference 1]. Figure 4 shows the stress-strain curves used for the materials, which were extracted from testing data [Reference 3]. An elastic-plastic material model was used in the finite element models. The service pipe was assumed to have the same material as the main pipe.

3. Validation study: Simulation of tapping tee test

This case simulated the load test under bending and tension on the main pipe and tapping tee assembly, which was performed experimentally to test the strength of the tapping tee [Reference 4]. Since experimental results are available to compare to, this case serves as a validation of the finite element model.

Figure 5 shows the model used for this case study. The top portion of the tapping tee was extended 2 inches as an approximation of the capped region. Half of the

structure was modeled to take advantage of the symmetry, with a symmetric boundary condition applied to the symmetry plane. The structure was loaded by prescribing a vertical motion to the outboard surface of the electrofusion coupling. The tapping tee was fixed at the bottom mating surface.

The model was meshed with quadratic tetrahedral elements (C3D10 in Abaqus). The mesh was refined in the lower corner region where the vertical and horizontal tubes of the tapping tee meet, where high local stresses were expected to develop. The finite element mesh of the model is shown in figure 6. The typical mesh size was 0.03 inch in the refined region and 0.1 inch elsewhere. The total number of elements in this case was 197,830 and the total number of degrees of freedom was 924,063.

Figure 7 shows the load-deflection curve from the simulation. Both the load and the deflection are measured at the centroid of the outboard surface of the electrofusion coupling, and are both in the vertical direction. The simulation was stopped when the load was 1976 lbs. This stopping point was chosen to be consistent with the experiment, where the load to fail the tapping tee at the service branch to valve body was 1966 lbs [Reference 4]. Figure 8 shows the deformed tapping tee structure at this load level.

Significant deformation is observed at the lower corner region where the vertical and horizontal tubes meet. Also, the top of the electrofusion coupling was in contact with the vertical tube, which contributes to the increase of stiffness in figure 7 when the deflection is above 1.6 inches. Both these observations are consistent with the tensile test [Reference 4]. Also shown in figure 8 is the contour plot of maximum principal logarithmic strain. The region with a value exceeding 1.6 was colored grey. A logarithmic strain of 1.6 represents the approximate failure strain of the tapping tee material [Reference 3]. It can be seen in figure 8 that the strain has reached this threshold in an extended area of the lower corner region. This indicates that the structure is likely to have failed at this point. Based on these results, it can be concluded that the finite element model behaves realistically and can be used to predict the deformation and failure behavior of the pipe assembly.

Note that a number of factors exist that preclude a higher level of correlation between simulation and experimental results. These factors include but are not limited to:

- Uncertainty in the direction and location of the applied load in the tensile test due to the load fixture, which used a cable to attach the testing machine crosshead to a clamp on the pipe at the edge of the electrofusion coupling [Reference 4]
- Boundary condition for restraint of the tapping tee: in the tensile test, the pipe assembly was tested with the section of the main pipe clamped to the base of the testing machine

- Rate-dependent behavior of the material: the mechanical testing of the tapping tee material was performed at a rate of 2.0 inch/min while the loading speed during the load test was 20 inch/min

An impact test was also performed on the tapping tee [Reference 4]. Experimental results showed that there was less plastic deformation when the structure failed due to dynamic impact. This result shows that the mechanical behavior of the tapping tee material is rate-dependent. Since no material data is available at the high rate comparable to what is experienced during a typical impact test, a simulation of the impact test was not performed. For the same reason, all subsequent simulations of possible failure scenarios were static simulations. More discussions on this matter can be found in later sections.

4. Case study A: Simulation of sagging of the main pipe

A series of case studies were performed with the finite element model. The main motivation was to study under simulated scenarios, whether the assumed preexisting separation would open, and whether a crack would develop in the lower corner region of the accident tapping tee (which corresponds to crack “c” in Reference 1 found in the accident tapping tee). The first case study focused on scenarios corresponding to sagging of the main pipe due to soil conditions.

a. Case 1: Vertical motion of the main pipe

This case simulated a scenario where the main pipe of the assembly experienced a downward vertical motion. For this case and all subsequent cases, the model of the pipe assembly as shown in figure 2 was used. The finite element mesh is shown in figure 9. The model was meshed with quadratic tetrahedral elements (C3D10 in Abaqus), except for the part of the horizontal tube that is away from the tapping tee, which was meshed with beam elements (B31 in Abaqus). The regions of the beam elements and solid elements were jointed via a coupling constraint (continuum coupling in Abaqus). The total number of elements in the model was 244,574 and the total number of degrees of freedom was 1,038,162.

To model the saddle fusion joint, a cohesive interface was created between the mating surfaces. The interfacial stiffness and strength were assumed to be the same as the pipe material. For the part of the interface that corresponds to the assumed preexisting separation (Regions 1 and 2 in Reference 1) as discussed earlier, an interfacial strength of zero was assumed.

To simulate this case, a vertical movement of 5 inches was applied to the ends of the main pipe segment. The main pipe was fixed at both ends for other degrees of freedom. The structure is also fixed at the end of the service pipe. The prescribed conditions are shown in figure 10.

Figure 11 shows the deformed shape of the structure after the main pipe was moved down 5 inches. It can be seen that the tapping tee is stressed at the lower corner

region. At the same time, the saddle fusion joint has opened at the assumed preexisting separation at the fusion interface. Figure 12 shows the contour plot of the contact opening at the joint interface and the maximum opening is about 0.02 inch.

Figure 13 shows the maximum principal logarithmic strain contour plot. The upper limit of the plot legend was chosen to be 1.15. It can be seen that strain in the lower corner region of the tapping tee shows evidence of a strain concentration, but the strain did not approach the failure strain (value of 1.6). It is also noted that the strain at the saddle fusion joint is not as high as the strain in the lower corner region of the tapping tee, indicating that there is no tendency for the assumed preexisting separation at the fusion interface to further expand in the fusion joint.

Figure 14 shows the contact pressure on the tapping tee side of the assumed preexisting separation in the saddle fusion joint. Dark red color highlights where there is positive contact pressure, which means the opposite surfaces of the joint are pressing together. It can be seen that the farther end of the region has positive contact pressure. This is further evidence that the joint interface does not have the tendency to completely open in this case. Instead, the opening of the joint seen in figure 11 is due to the tapping tee arching upward.

This case indicates that vertical motion of the pipe can stress the tapping tee lower corner without further expanding the assumed preexisting separation along part of the saddle fusion interface. But it takes a movement considerably larger than 5 inches to achieve a strain that is enough to create a failure in the lower corner region of the tapping tee.

b. Case 2: Bending of the main pipe

This case simulated a scenario of downward bending of the main pipe. A rotation was applied at the ends of the main pipe segment while keeping the ends in place. In addition, the service pipe was fixed at its end. Figure 15 shows the prescribed conditions of this case.

Figure 16 shows the deformed shape of the pipe assembly when the deflection at the mid-point of the main pipe was approximately 5 inches. It can be seen that the assumed preexisting separation at the saddle fusion interface has a tendency to open up in this case. The peak opening in figure 16 exceeded 0.1 inch. Figure 17 shows the maximum principal logarithmic strain contour plot. It can be seen that the saddle fusion joint has a higher strain than the tapping tee lower corner. Hence, this case indicates that when downward bending motion is applied to the main pipe, the assumed preexisting separation at the saddle fusion interface will tend to open up and eventually fail before the tapping tee.

5. Case study B: Simulation of possible post-accident excavation activities

The second case study focused on scenarios where the pipe assembly is deformed by external forces that the pipe assembly could experience during post-accident excavation activities.

a. Case 3: Pushing the tapping tee down from top

This case simulated a scenario where the tapping tee was moved 7 inches vertically down. The motion was applied to the top surface of the tapping tee. The main pipe was allowed to move vertically but was constrained at the ends for all other degrees of freedom. Figure 18 shows the prescribed conditions.

Figure 19 shows the maximum principal logarithmic strain contour plot. It can be seen that the deformation mode of this case is very similar to that of Case 1. High strains develop at the lower corner of the tapping tee due to bending. The assumed preexisting separation does not show a tendency to completely open, although localized strain does develop at the interface due to the tapping tee rotating with respect to the main pipe. From figure 19 it can be seen that at a downward movement of 7 inches, the strain at the lower corner of the tapping tee still did not reach the failure threshold. However this only means that a static failure may not be possible at the prescribed displacement. As previously discussed, failure under dynamic impact may be possible due to the possibility of a lower failure strain threshold at a higher rate.

This case indicates that pushing the tapping tee down can stress the tapping tee lower corner without further opening up the assumed preexisting separation at the saddle fusion interface.

b. Case 4: Bending the tapping tee at top

This case simulated a scenario where the tapping tee was bent outwards away from the service pipe, which is an idealization of an outward lateral force hitting the tapping tee on the top. The motion was applied to the top surface of the tapping tee. The top surface was also rigidly constrained to simulate the added stiffness of the cap and the cutter. The main pipe segment was fixed at its ends. Figure 20 shows the prescribed conditions.

Figure 21 shows the deformed shape and maximum principal logarithmic strain contour plot of the structure when the top of the tapping tee moved approximately 0.8 inch outwardly. It can be seen that in this scenario higher strains developed at the upper corner, as opposed to the lower corner of the tapping tee. Based on this result, this case indicates that it is unlikely that a bending moment or a horizontal force at the top of the tapping tee in the direction shown could cause it to fail in the lower corner region.

c. Case 5: Pushing the service pipe up near the tapping tee outlet

This case simulated a scenario where the service pipe was pushed up near the tapping tee outlet, which is an idealization of possible motion the assembly experienced during post-accident excavation. In the finite element model, a uniformly distributed pressure was applied to the bottom of the service pipe near the tapping tee outlet. The service pipe and the main pipe were fixed at their ends. Figure 22 shows the prescribed conditions.

Figure 23 shows the deformed shape of the assembly at an applied force of 1550 pounds. Figure 24 shows the maximum principal logarithmic strain contour plot. It can be seen that strain in the lower corner region of the tapping tee shows evidence of a strain concentration, indicating that it may become the first location to fail with increasing load. High strain can also be seen developing on top of the service pipe where bending occurred. This indicates that the structure may develop notable permanent deformation on the service pipe under this deformation mode. Stress concentration is also noted at the saddle fusion interface indicating propagation of the assumed preexisting area of separation under increasing load.

d. Case 6: Pushing the main pipe horizontally away from the service pipe

This case simulated a scenario where the main pipe was pushed horizontally away from the service pipe, which is an idealization of possible motion the assembly experienced during post-accident excavation. The motion was applied to the two ends of the main pipe segment while keeping those ends in their original planes. The service pipe was fixed at its end. Figure 25 shows the prescribed conditions.

Figure 26 shows the deformed shape of the assembly at a horizontal displacement of 4.3 inches. The applied horizontal force was 1300 pounds at this displacement. Figure 27 shows the maximum principal logarithmic strain contour plot. The region with a value exceeding 1.6, which is the failure strain threshold, was colored grey. It can be seen that areas at the lower corner of the tapping tee experienced a level of deformation that exceeded the failure threshold. At the same time, the assumed preexisting separation at the saddle fusion interface remained closed.

6. Case study C: Simulation of sagging of the main pipe under more severe in-service conditions

The third case study re-visited the scenario of sagging of the main pipe with the model revised to reflect more severe, static load conditions such as those from the dirt/pavement overburden.

a. Case 7: Sagging of the main pipe with the tapping tee at mid-span

For this case, the model was modified to include 20 feet of the main pipe. Based on the accident investigation, it was reasonable to assume that sagging could only happen for this portion of the main pipe and fixed boundary conditions were applied to

the ends of the main pipe segment to reflect this assumption. The model was also modified to include 16 inches of the service pipe. Based on the accident investigation, it was reasonable to assume solid soil support on the service pipe beyond this 16-inch region and hence fixed boundary conditions were applied to the ends of the service pipe segment. The tapping tee was placed at the mid-span of the main pipe. A uniformly distributed vertical load was applied to the top surface of the main pipe to simulate the load that the main pipe could experience during service. The magnitude of the loading was chosen to be 135 lbs/ft. Figure 28 shows the modified model geometry and the prescribed conditions. The revised model contains 273,436 elements and 1,094,622 degrees of freedom.

Figure 29 shows the deformed shape of the structure. Figure 30 shows the maximum principal logarithmic strain contour plot in the vicinity of the tapping tee. The upper limit of the plot legend was chosen to be 1.6, which is the failure strain threshold. Strain concentration can be seen at the lower corner region of the tapping tee. The peak strain was about 1.33 and did not exceed 1.6. This indicated that a crack was unlikely to initiate in the region. Figure 30 shows that an opening developed at the saddle fusion interface due to the assumed preexisting separation. The maximum opening was measured to be approximately 0.05 inches. Table 2 summarizes the opening at the assumed preexisting separation interface at various main pipe deflection values.

Table 2. Case 7: Opening at the preexisting separation vs. Main pipe deflection.

Main pipe deflection due to sagging (inch)	Opening at the assumed preexisting separation (inch)
2.0	0.02
3.6	0.04
7.2	0.05

b. Case 8: Sagging of the main pipe with the tapping tee offset from mid-span

For this case, model 7 was modified by offsetting the tapping tee by one foot to the south (direction as used in Reference 1). Figure 31 shows the modified model geometry. The other parts of the model remained unchanged.

Figure 32 shows the maximum principal logarithmic strain contour plot in the vicinity of the tapping tee. Similar to the previous case, the upper limit of the plot legend was chosen to be 1.6. Strain concentration can be seen at the lower corner region of the tapping tee. The peak strain was again about 1.33 and did not exceed 1.6. This indicated that a crack was unlikely to initiate in the region. Figure 33 shows that an opening developed at the saddle fusion interface due to the assumed preexisting separation. The maximum opening was measured to be approximately 0.06 inches. Table 3 summarizes the opening at the assumed preexisting separation interface at various main pipe deflection values.

Table 3. Case 8: Opening at the preexisting separation vs. Main pipe deflection.

Main pipe deflection due to sagging (inch)	Opening at the assumed preexisting separation (inch)
1.5	0.02
3.4	0.04
7.2	0.06

c. Case 9: Sagging of the main pipe with a bigger assumed preexisting separation area at the saddle fusion interface

For this case, the assumed preexisting separation at the saddle fusion interface was enlarged to include an arc of 240 degrees, which corresponds to Regions 1 through 3 in Reference 1. The motivation for this change is that it was possible for the crack to have propagated into region 3 during the pipe assembly's service time. Figure 34 shows the modeled area of separation, with comparison to the photograph of the actual saddle fusion fracture surface. The other parts of the model remained unchanged from Case 8.

Figure 35 shows the maximum principal logarithmic strain contour plot in the vicinity of the tapping tee. Similar to the previous two cases, the upper limit of the plot legend was chosen to be 1.6. Strain concentration can be seen at the lower corner region of the tapping tee. The peak strain was about 1.31 and did not exceed 1.6. This indicated that a crack was unlikely to initiate in the region. Figure 36 shows that an opening developed at the saddle fusion interface due to the assumed preexisting separation. The maximum opening for this case was measured to be approximately 0.13 inches. Table 4 summarizes the opening at the assumed preexisting separation at various main pipe deflection values.

Table 4. Case 9: Opening at the preexisting separation vs. Main pipe deflection.

Main pipe deflection due to sagging (inch)	Opening at the assumed preexisting separation (inch)
1.3	0.03
2.8	0.09
7.2	0.13

7. Summary

From the exploratory evaluations of the case studies chosen, the following conclusions can be drawn:

1. Movement of the main pipe due to sagging could be a combination of vertical motion and bending. Based on the results from Case 1 and 2, it is unlikely that this was the cause of the crack in the tapping tee. The reasons are: a. the required motion to reach failure strain is large and b. under such a motion, the

- fusion saddle joint will open and the assumed preexisting separation at the saddle fusion interface would likely expand before a crack developed at the lower corner of the tapping tee.
2. Based on the results from Case 3, applying a downward force to the top of the tapping tee in a static fashion is unlikely to cause a crack in the tapping tee under realistic conditions. However a downward dynamic impact force may be able to do so.
 3. Based on the results from Case 4, it is unlikely to initiate a crack in the tapping tee at its lower corner region by applying a bending moment or horizontal force to the top of the tapping tee to move it away from the service pipe.
 4. Based on the results from Case 5, it is possible to initiate a crack in the tapping tee at its lower corner region by pushing the service pipe up at the tapping tee, although this motion will also cause notable permanent deformation in the service pipe.
 5. Based on the results from Case 6, it is possible to initiate a crack in the tapping tee at its lower corner region by applying an outward horizontal motion to the main pipe. The assumed preexisting separation at the saddle interface remains closed under that scenario.
 6. Based on the results from Case 7 through 9, it is unlikely to initiate a crack in the tapping tee at its lower corner region under the assumed worst-case in-service sagging situations. However, the assumed preexisting separation at the saddle interface has the tendency to open under the same situations. The opening can be considerably bigger if the assumed preexisting separation is expanded to include region 3 in Reference 1.

D. REFERENCES

1. Materials Laboratory Factual Report 14-069, Accident DCA14MP002, National Transportation Safety Board, Washington, DC, 2014.
2. Frialen Safety Fittings Product Catalog, Friatec.
3. Tensile testing report, Intertek Plastics Technology Laboratories.
4. Materials Laboratory Factual Report 14-086, Accident DCA14MP002, National Transportation Safety Board, Washington, DC, 2014.

Xiaohu Liu
Finite Element Analyst

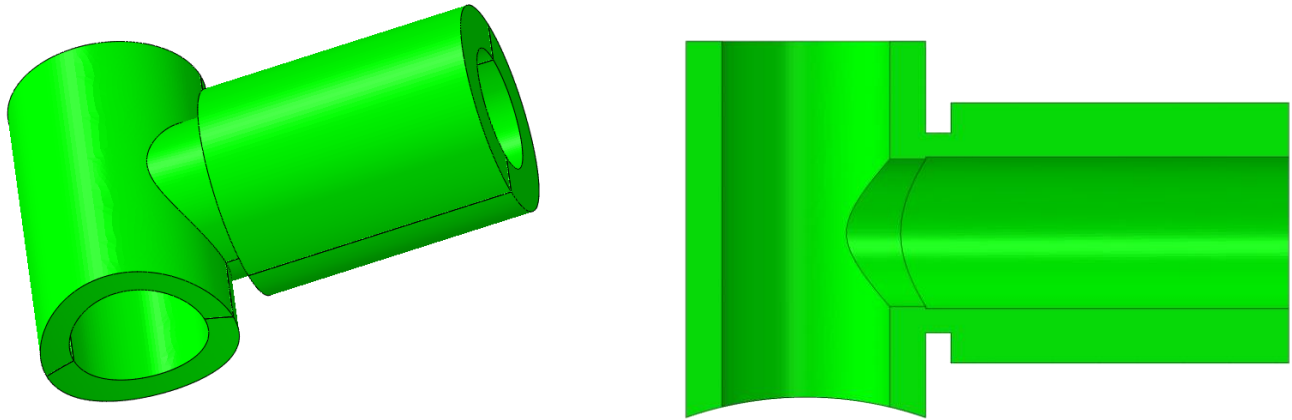


Figure 1. Geometry of the tapping tee/electrofusion coupling model.

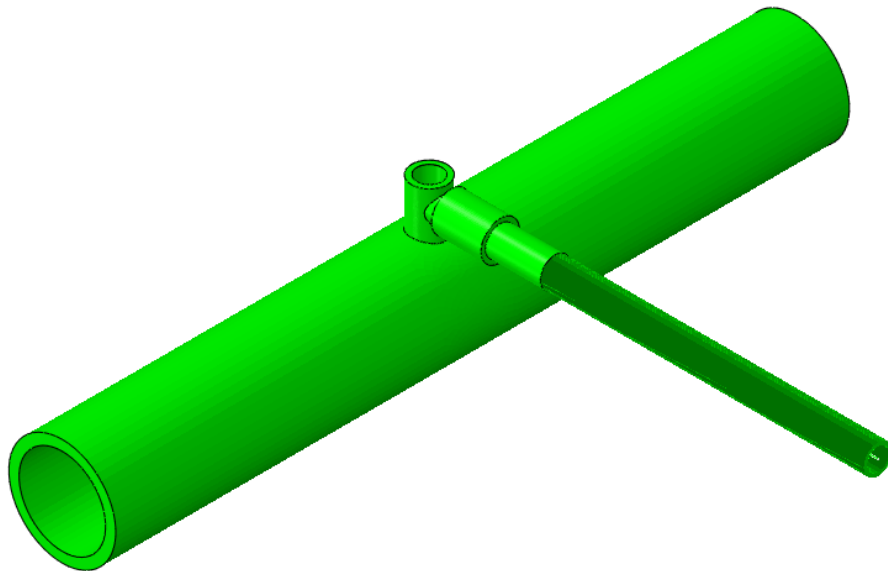


Figure 2. Geometry of the pipe assembly model.

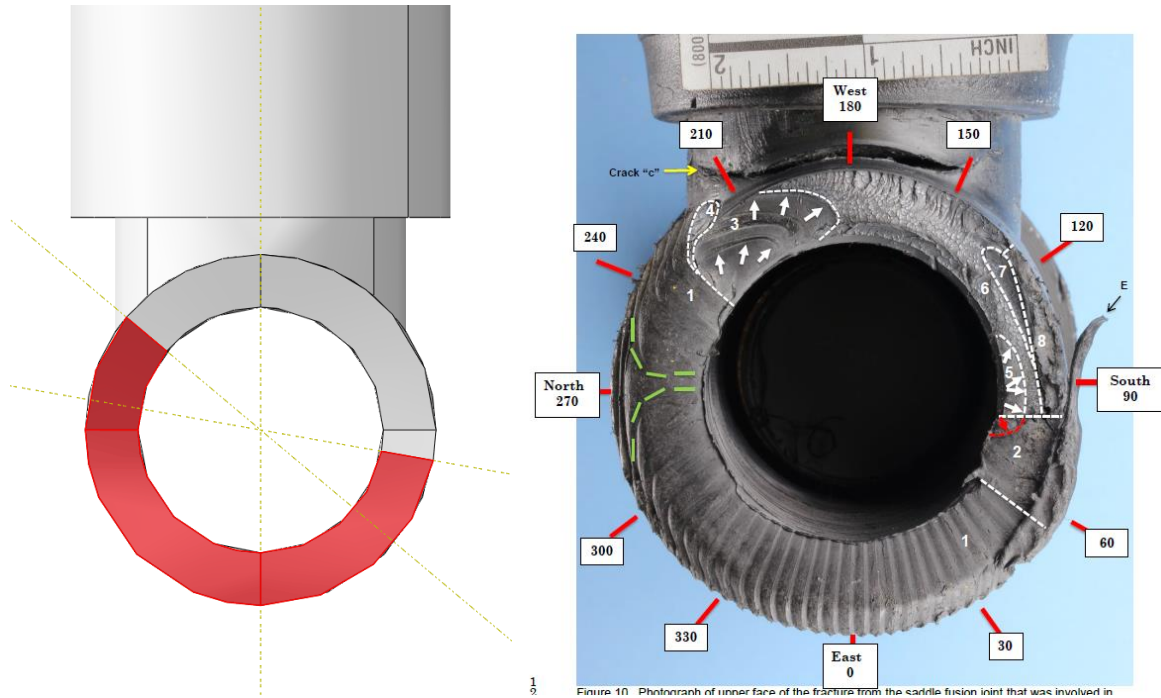


Figure 3. The saddle fusion joint interface (with assumed region of preexisting separation shown in red) compared to a photograph of the accident tapping tee (figure 10 of Reference 1).

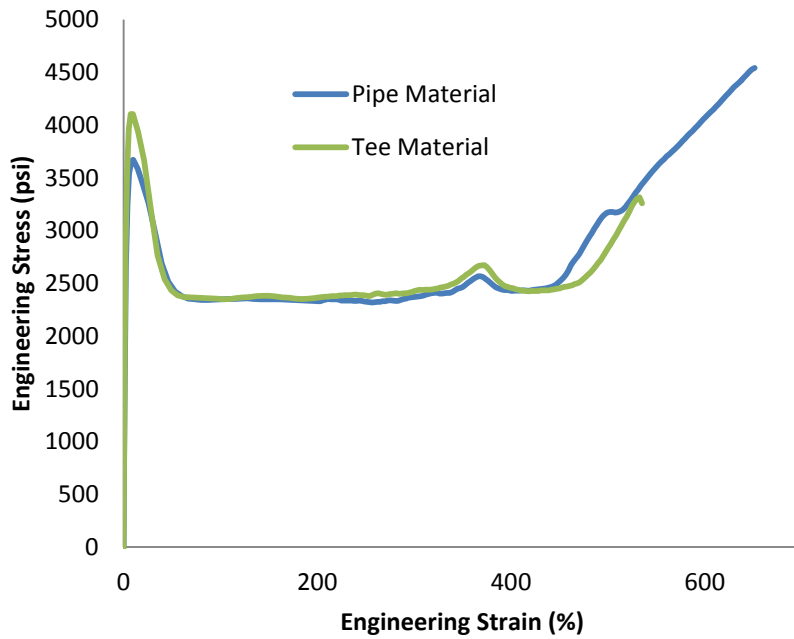


Figure 4. Stress-strain curves of the main pipe and tapping tee material.

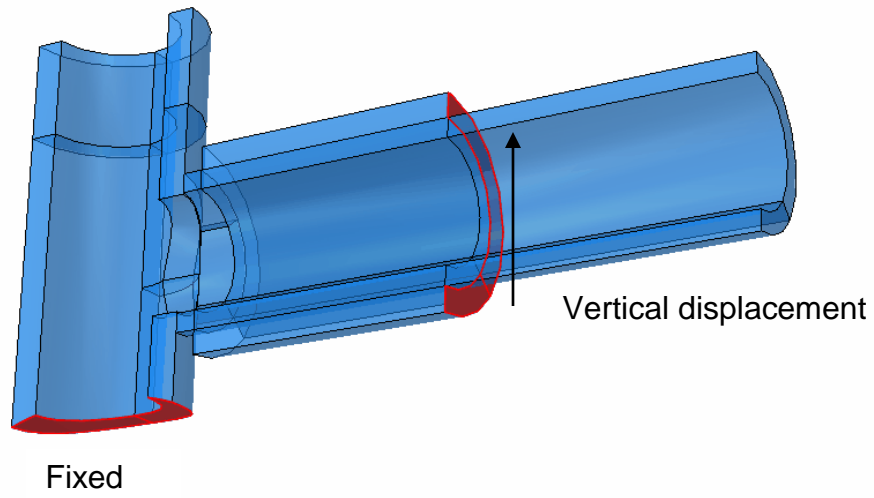


Figure 5. Geometry and boundary conditions for the tapping tee tensile test model.

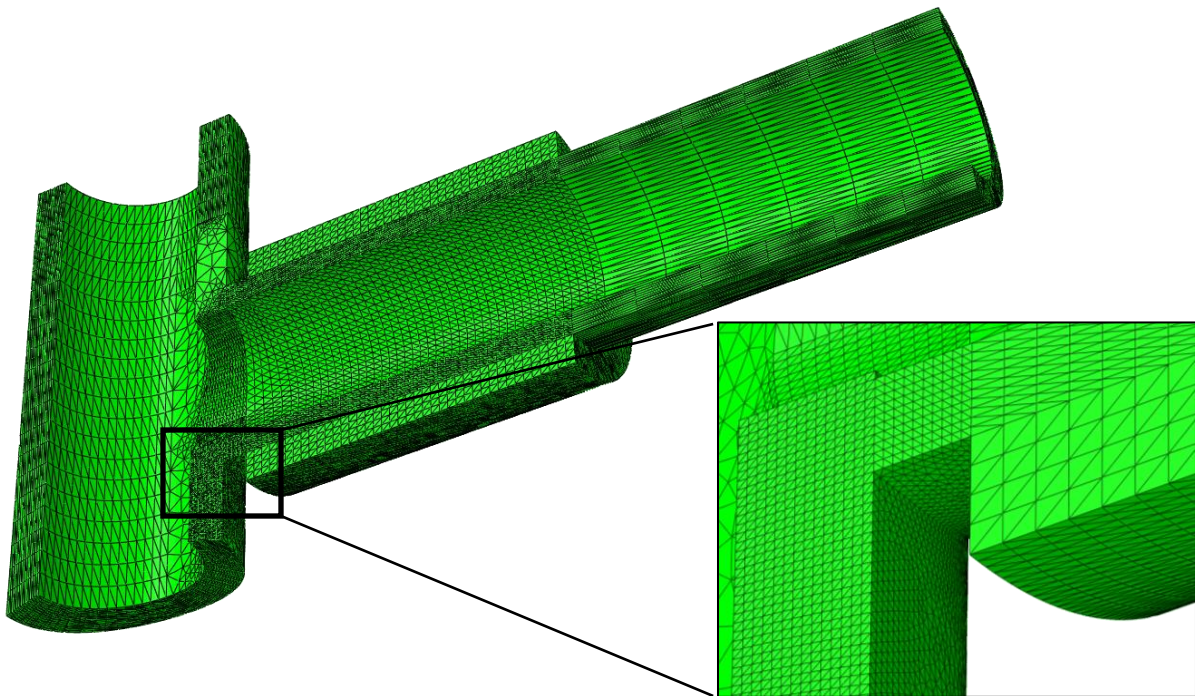


Figure 6. Finite element mesh of the tapping tee model.

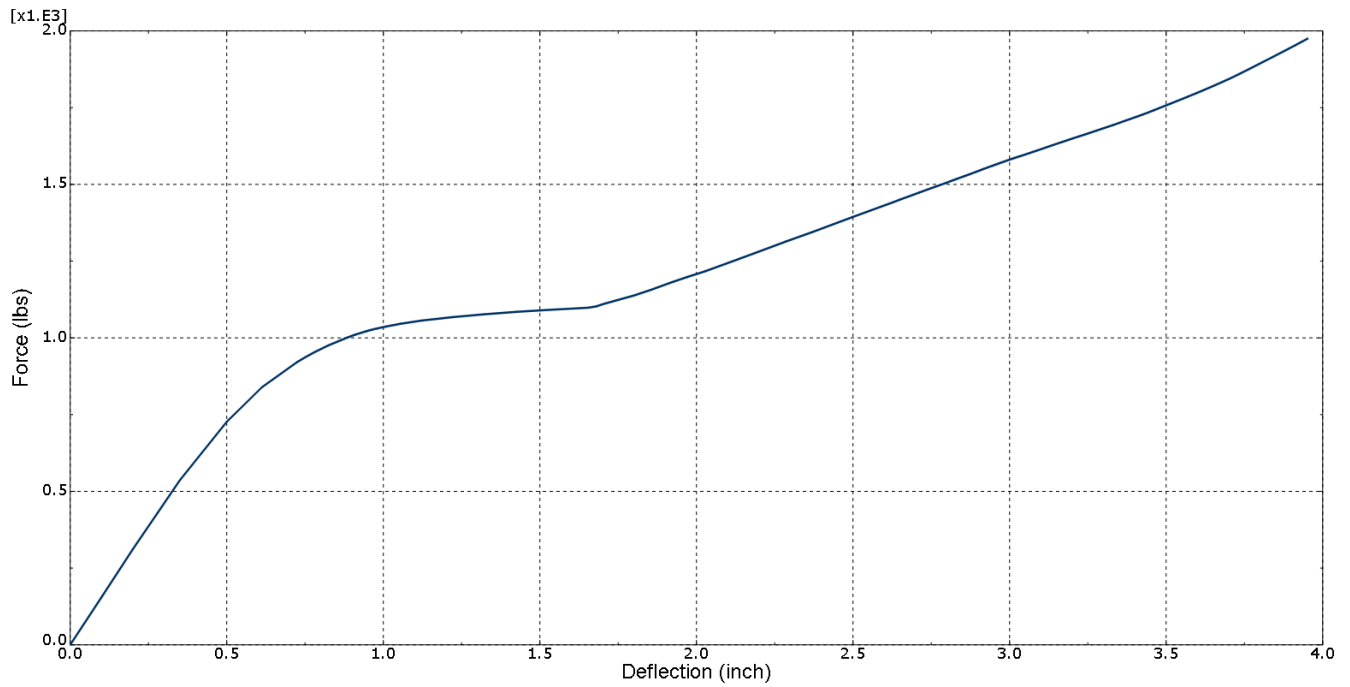


Figure 7. Force-deflection curve of the simulated tapping tee tensile test.

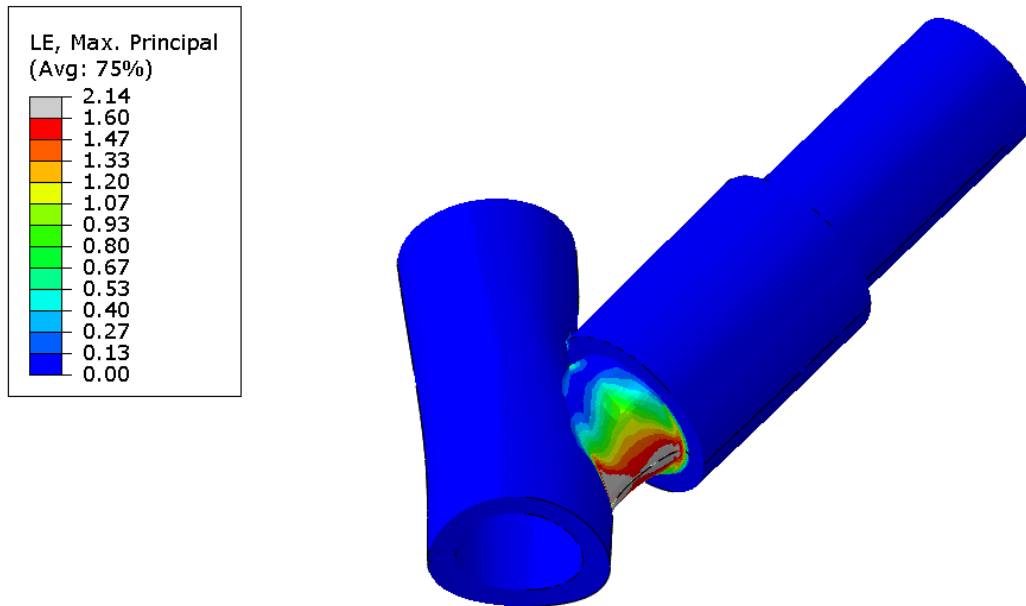


Figure 8. Deformed shape and maximum principal logarithmic strain contour plot of the tapping tee tensile test simulation.

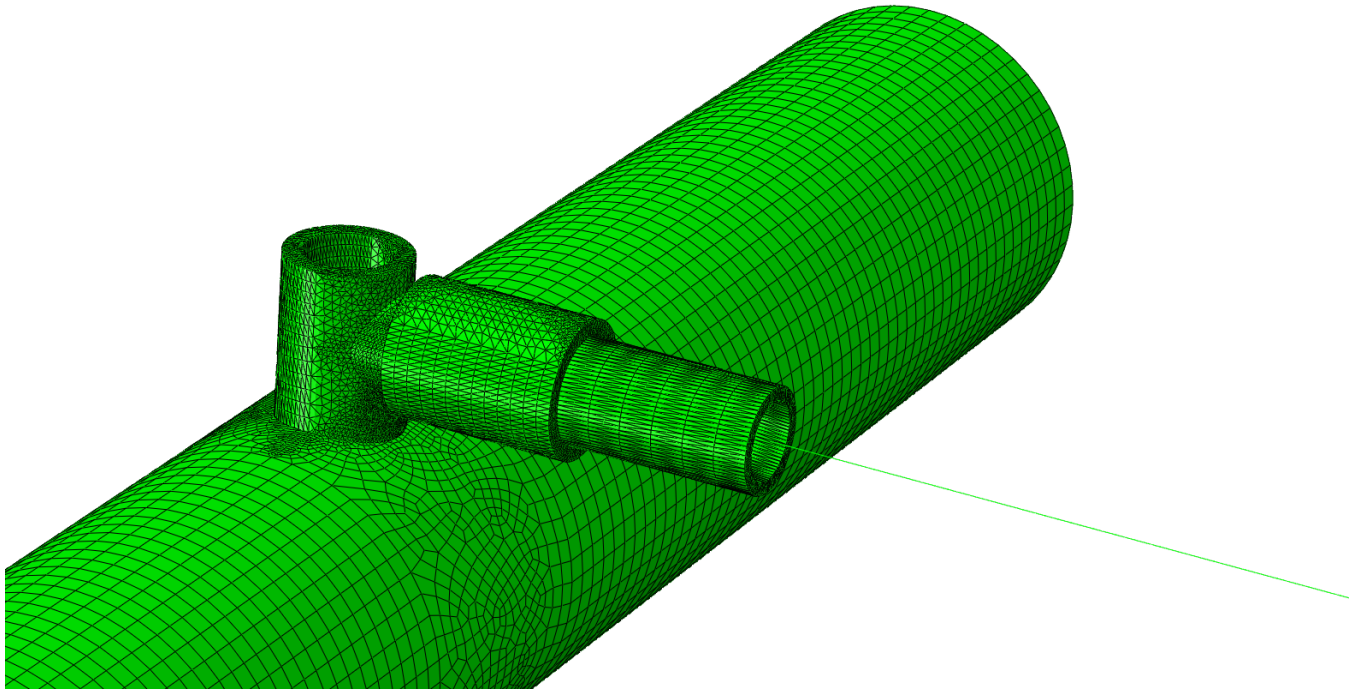


Figure 9. Finite element mesh of the pipe assembly model.

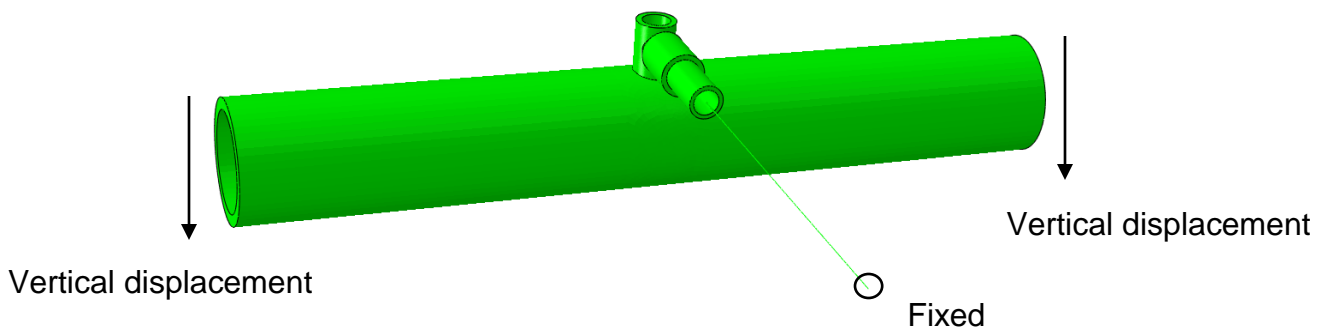


Figure 10. Case 1: Prescribed conditions.

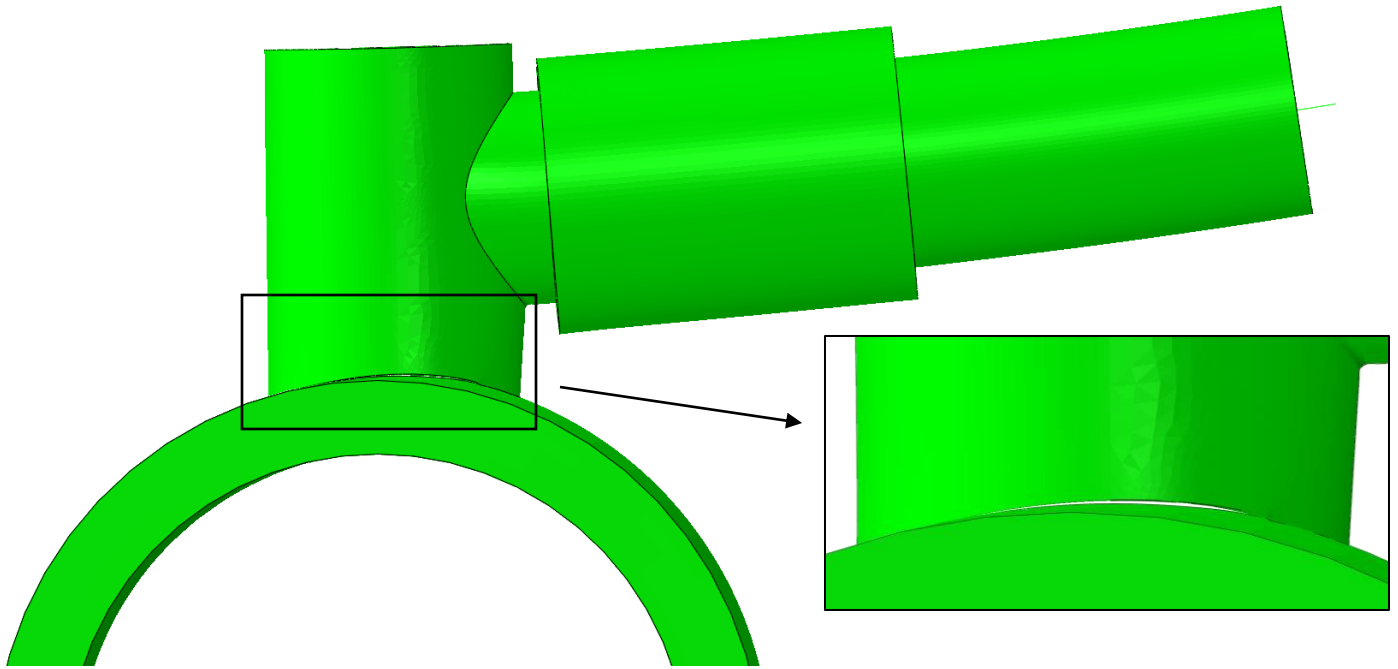


Figure 11. Case 1: deformed shape of the structure.

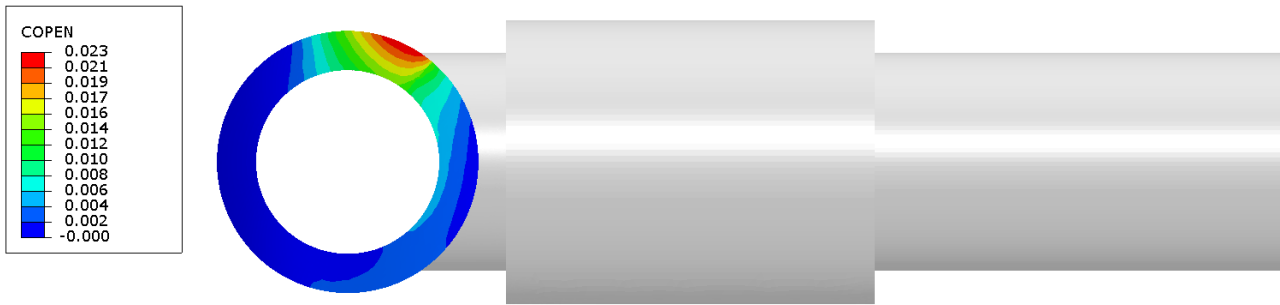


Figure 12. Case 1: Contact opening at the saddle fusion joint interface (unit: inch)

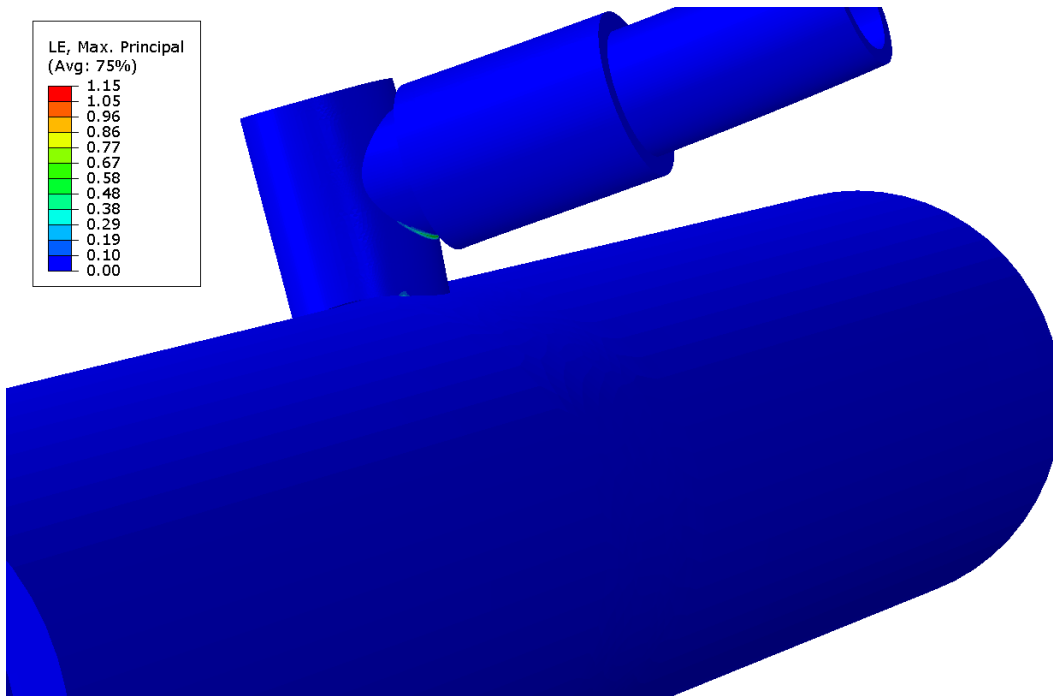


Figure 13. Case 1: Contour plot of maximum principal logarithmic strain.



Figure 14. Contact pressure at the assumed preexisting separation at the saddle fusion interface (unit: psi).

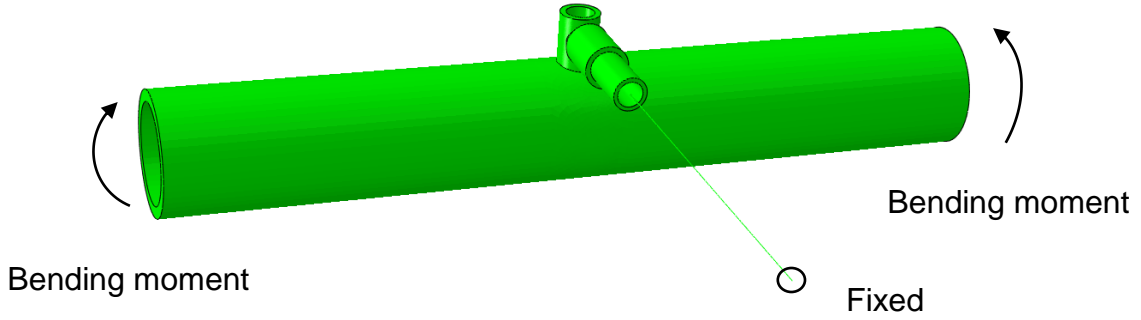


Figure 15. Case 2: Prescribed conditions.

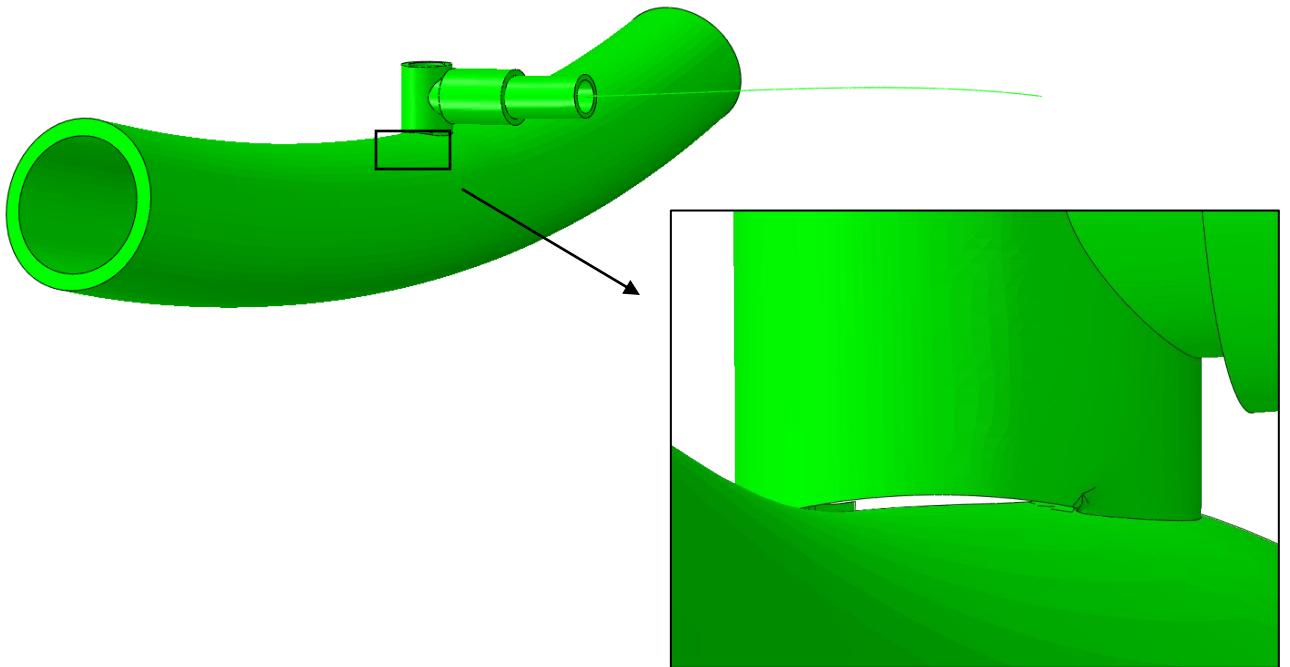


Figure 16. Case 2: Deformed shape.

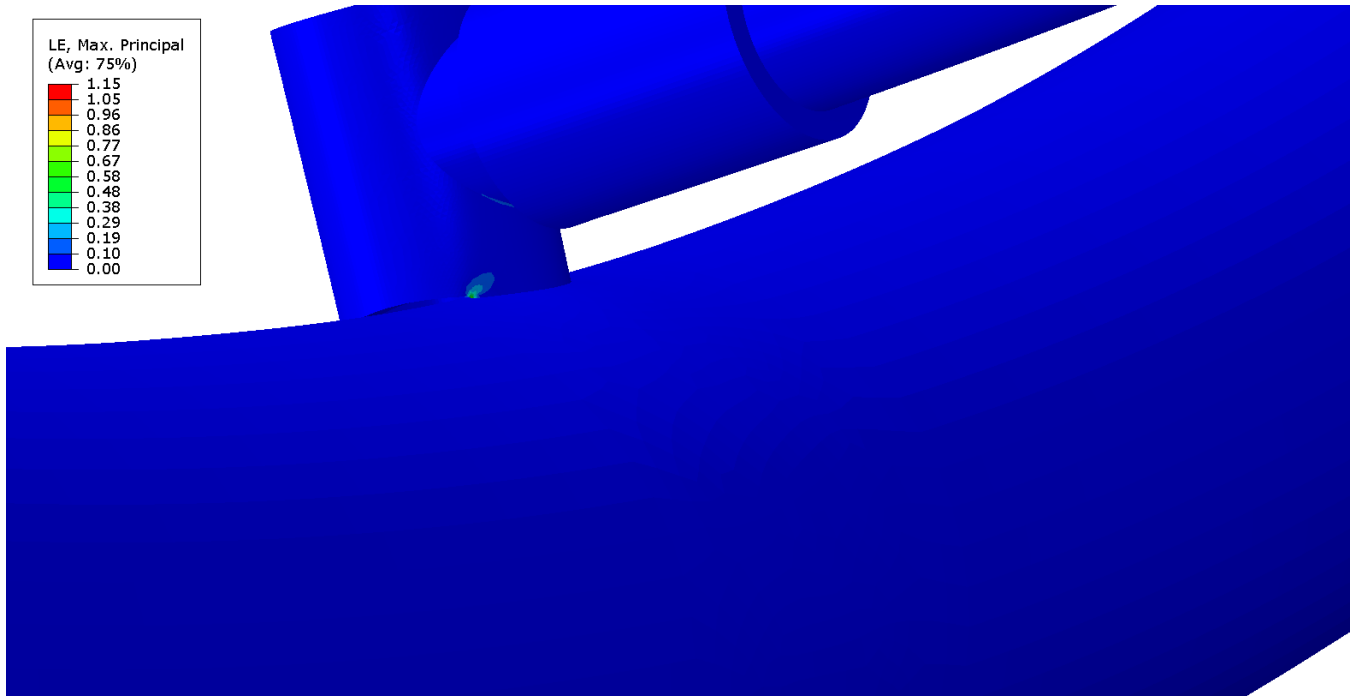


Figure 17. Case 2: Contour plot of maximum principal logarithmic strain.

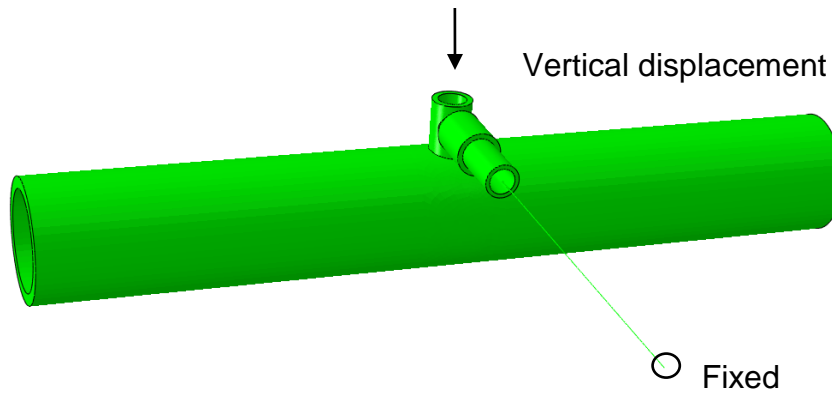


Figure 18. Case 3: Prescribed conditions.

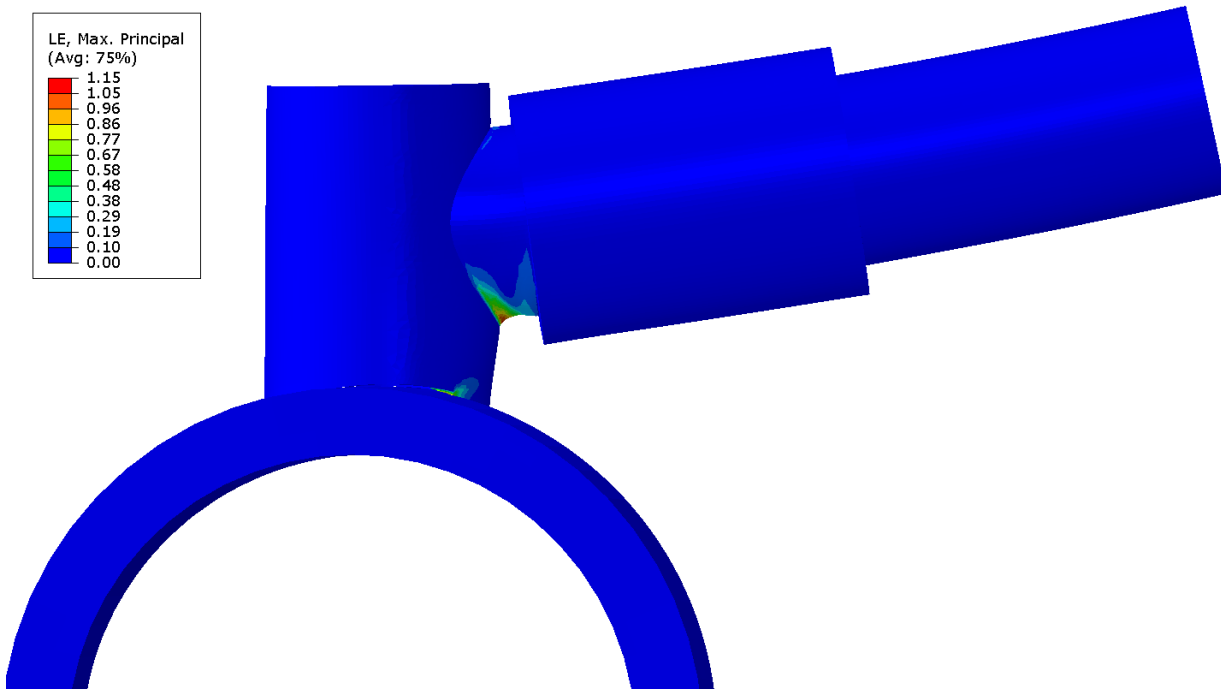


Figure 19. Case 3: Contour plot of maximum principal logarithmic strain.

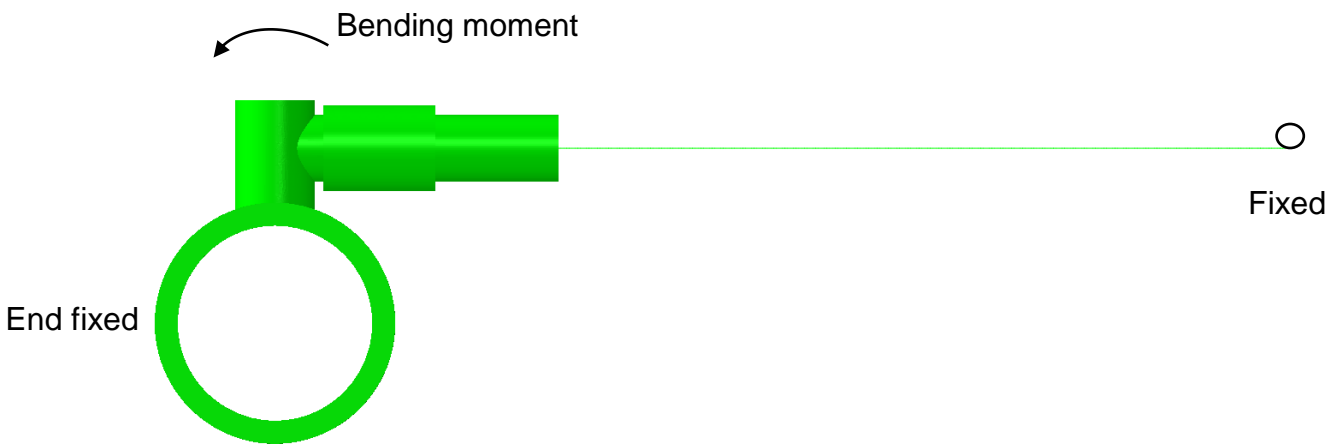


Figure 20. Case 4: Prescribed conditions.

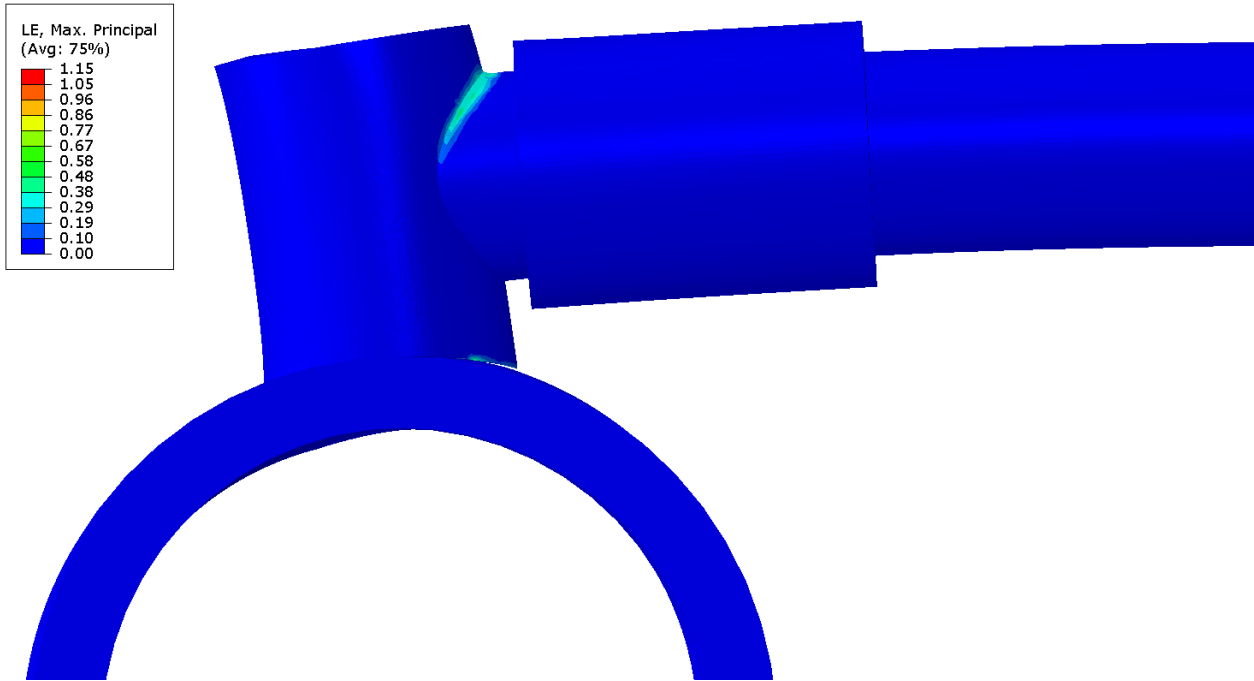


Figure 21. Case 4: Contour plot of maximum principal logarithmic strain.

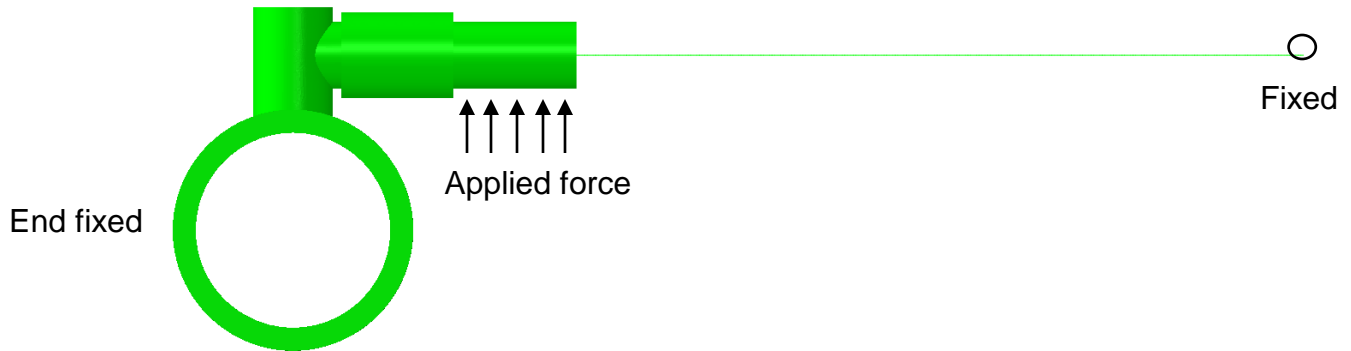


Figure 22. Case 5: Prescribed conditions.

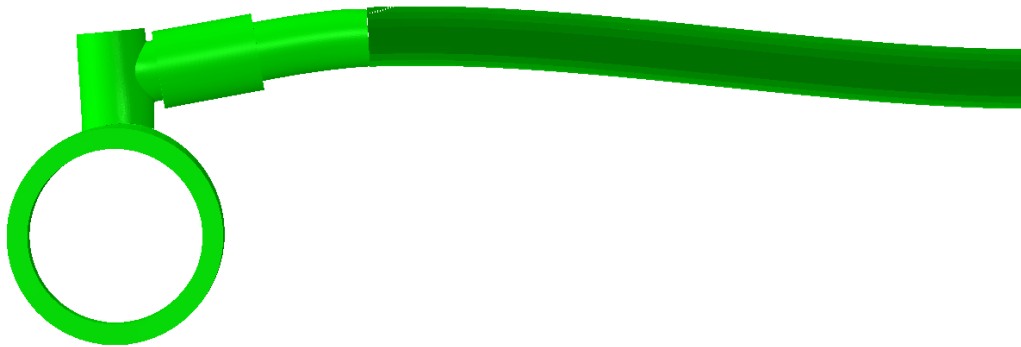


Figure 23. Case 5: Deformed shape of the structure.

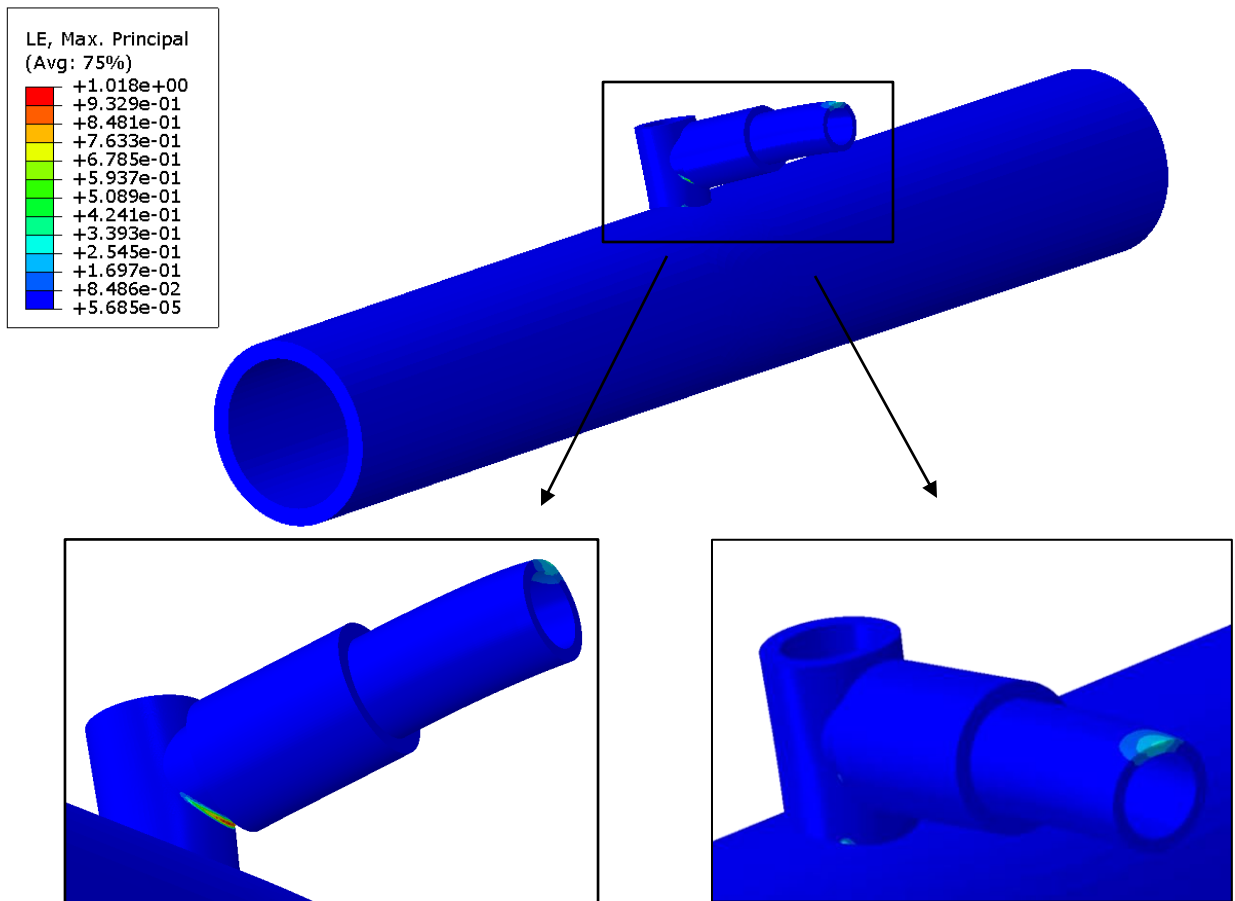


Figure 24. Case 5: Contour plot of maximum principal logarithmic strain.

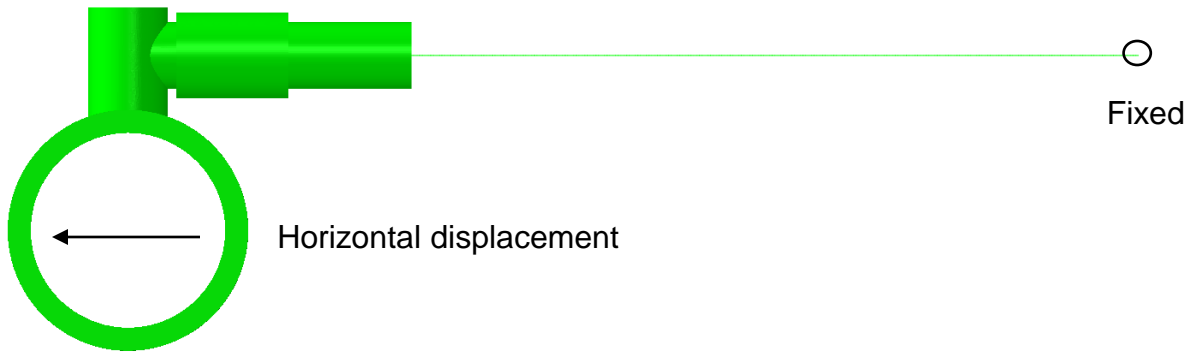


Figure 25. Case 6: Prescribed conditions.

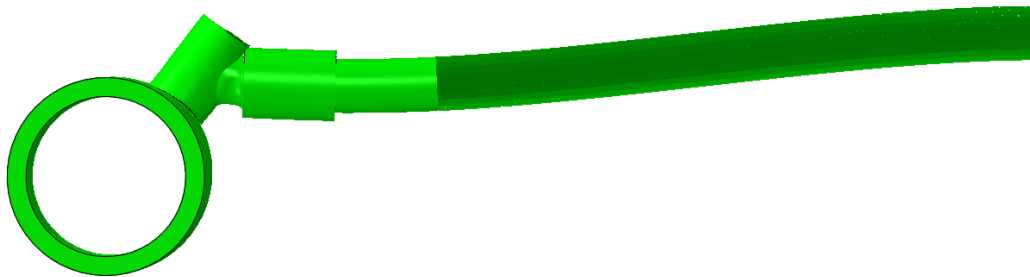


Figure 26. Case 6: Deformed shape of the structure.

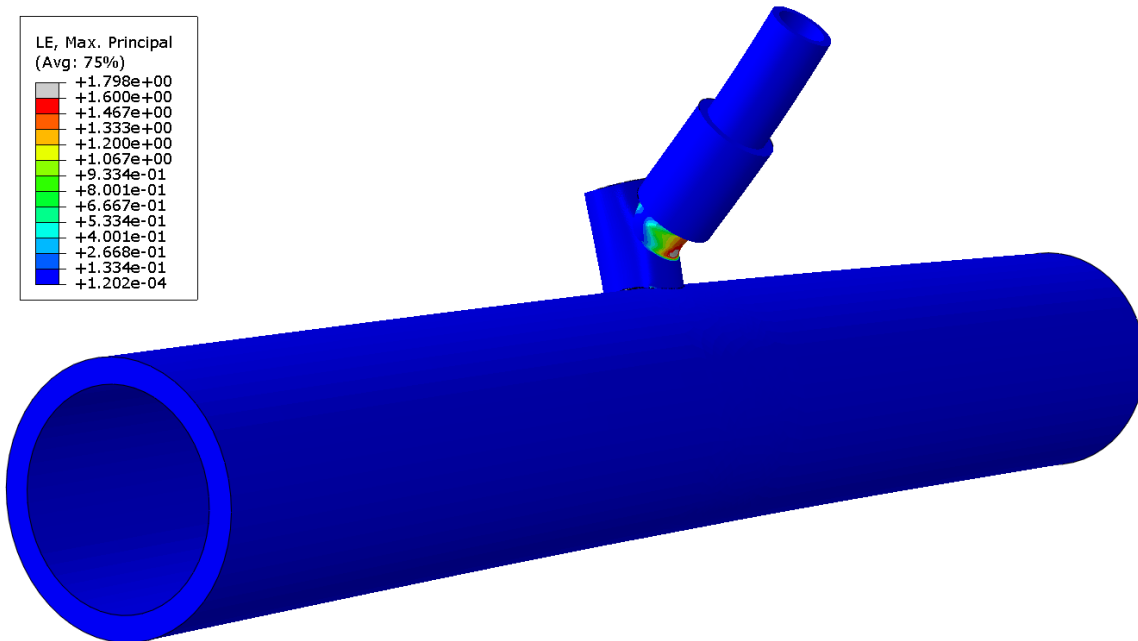


Figure 27. Case 6: Contour plot of maximum principal logarithmic strain.

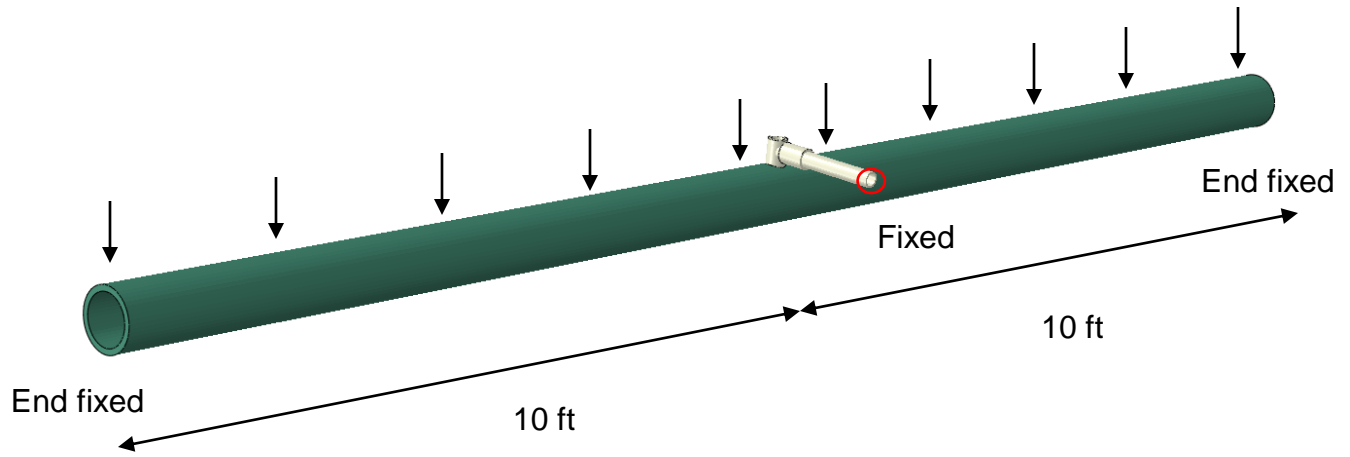


Figure 28. Case 7: Model geometry and prescribed conditions.

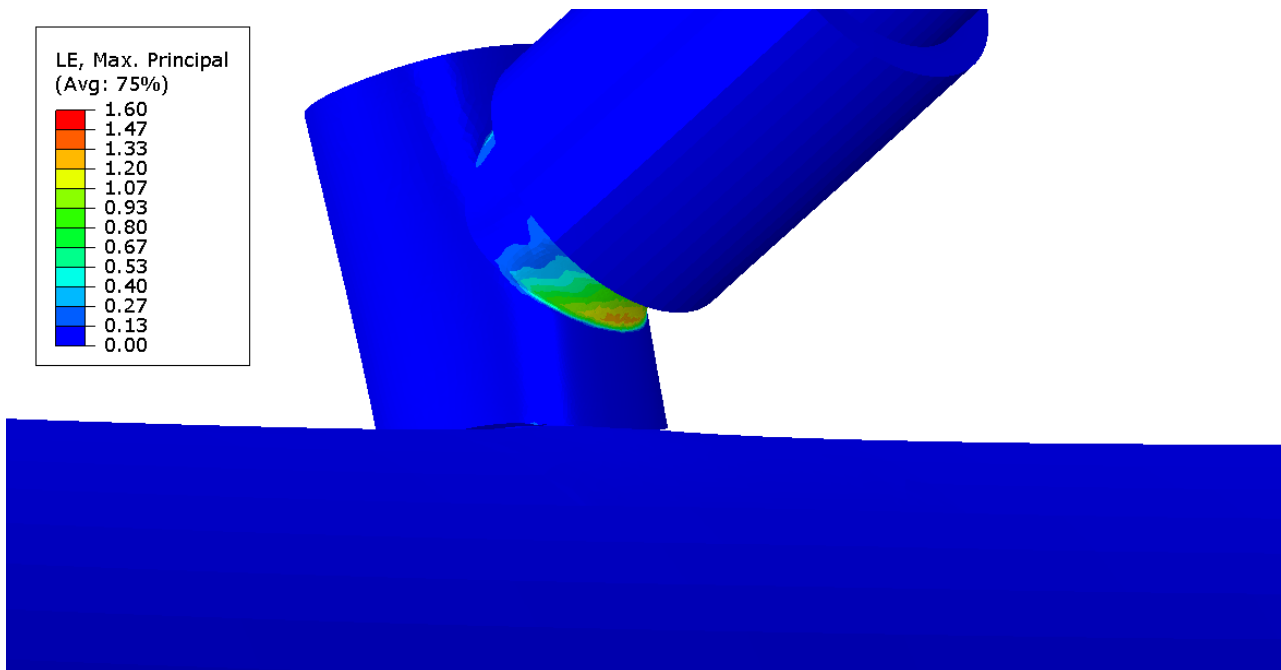


Figure 29. Case 7: Contour plot of maximum principal logarithmic strain.

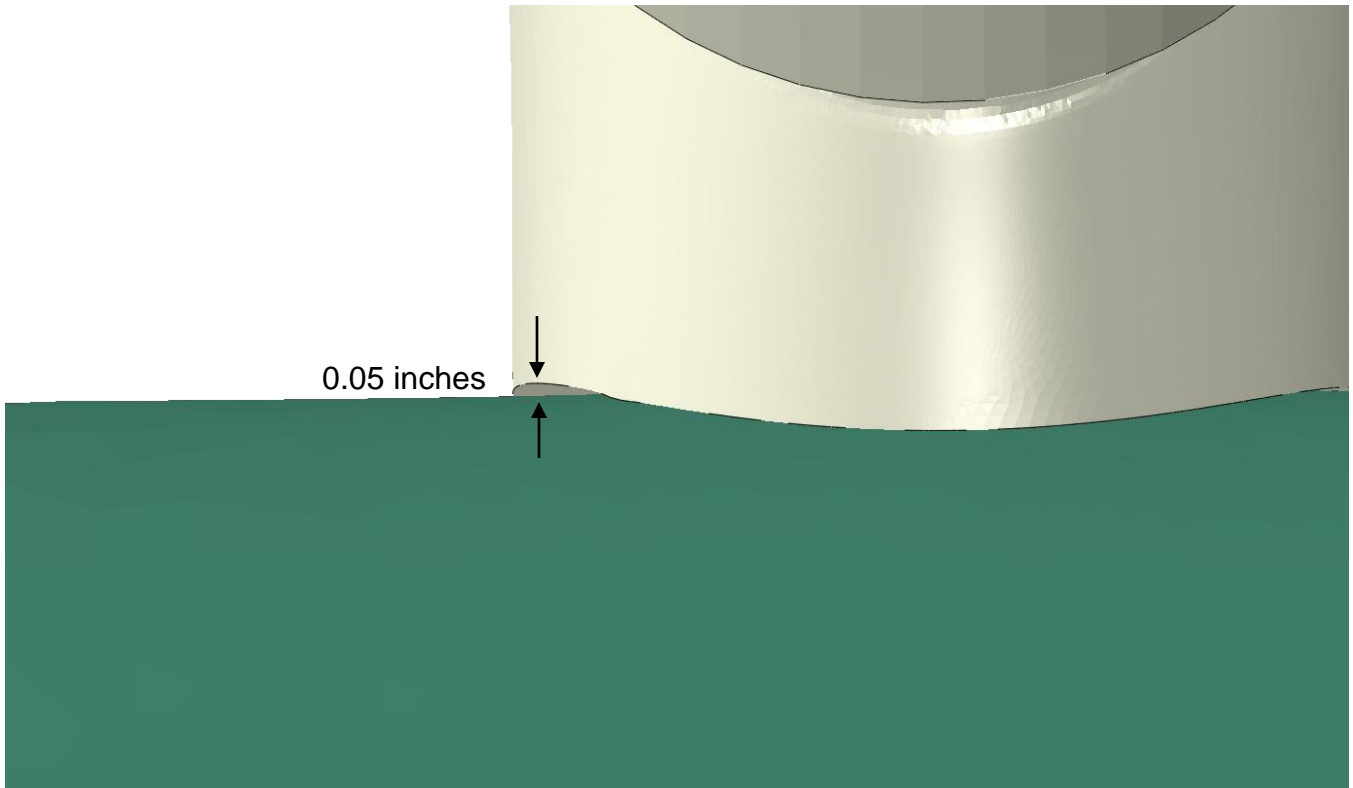


Figure 30. Case 7: Opening at the saddle fusion interface.

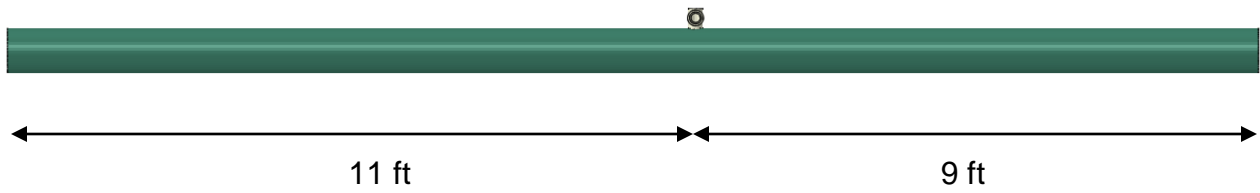


Figure 31. Case 8: Model geometry.

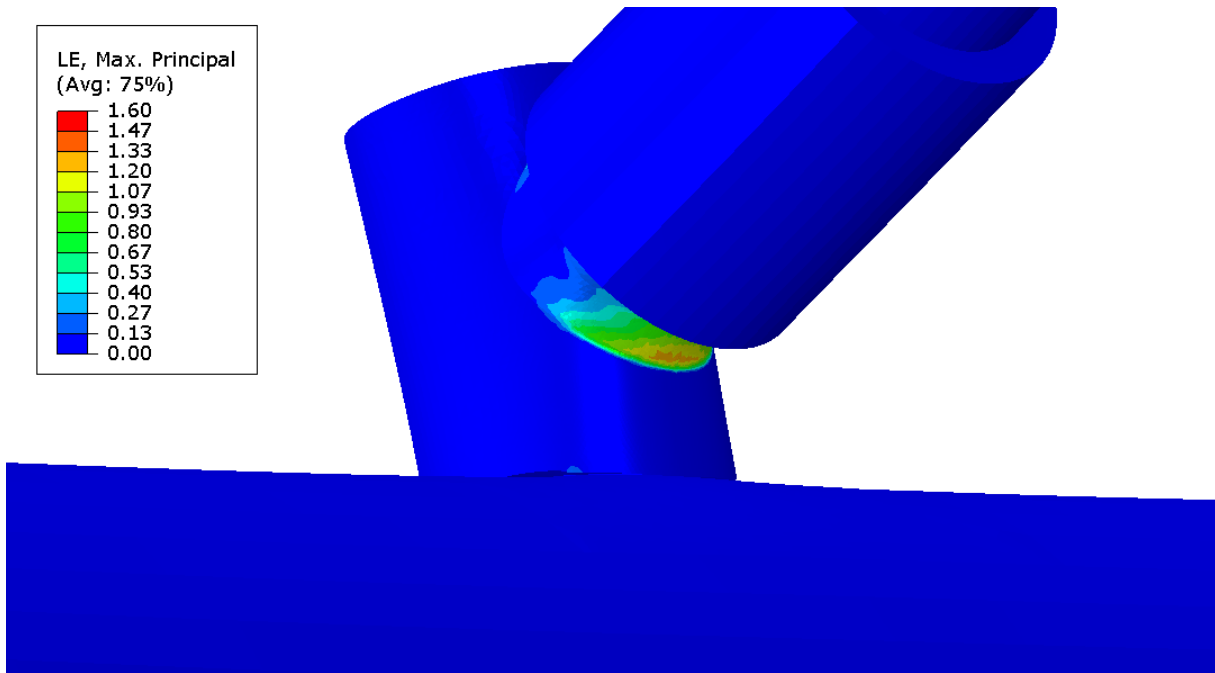


Figure 32. Case 8: Contour plot of maximum principal logarithmic strain.

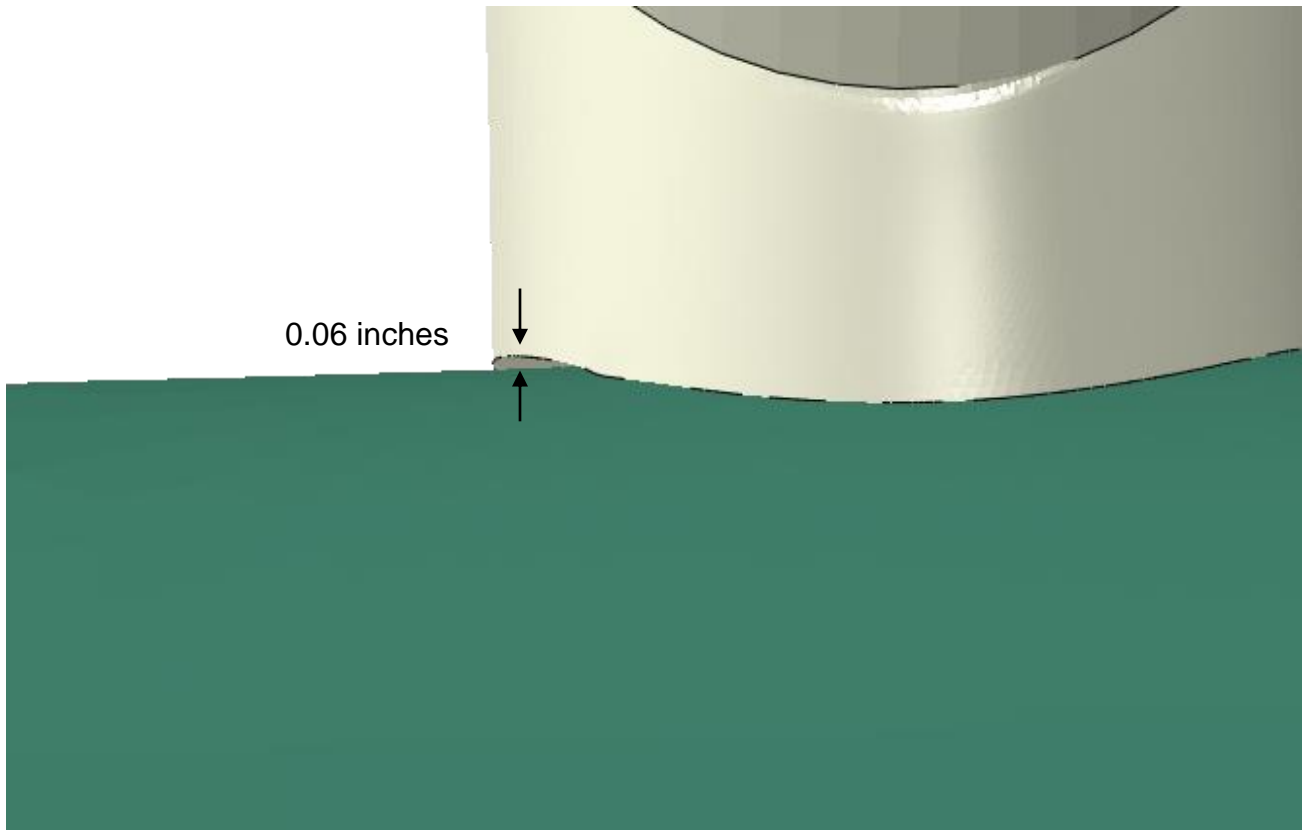


Figure 33. Case 8: Opening at the saddle fusion interface.

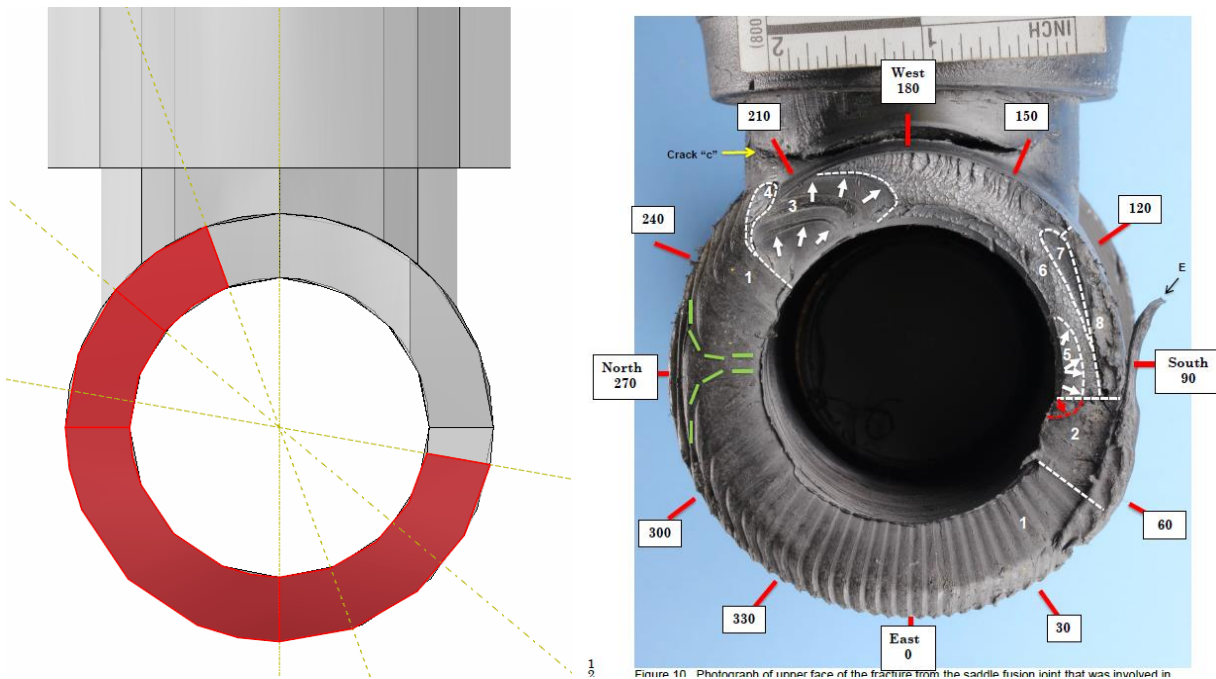


Figure 34. The saddle fusion joint interface modeled in Case 9 (with assumed region of preexisting separation shown in red) compared to a photograph of the accident tapping tee (figure 10 of Reference 1).

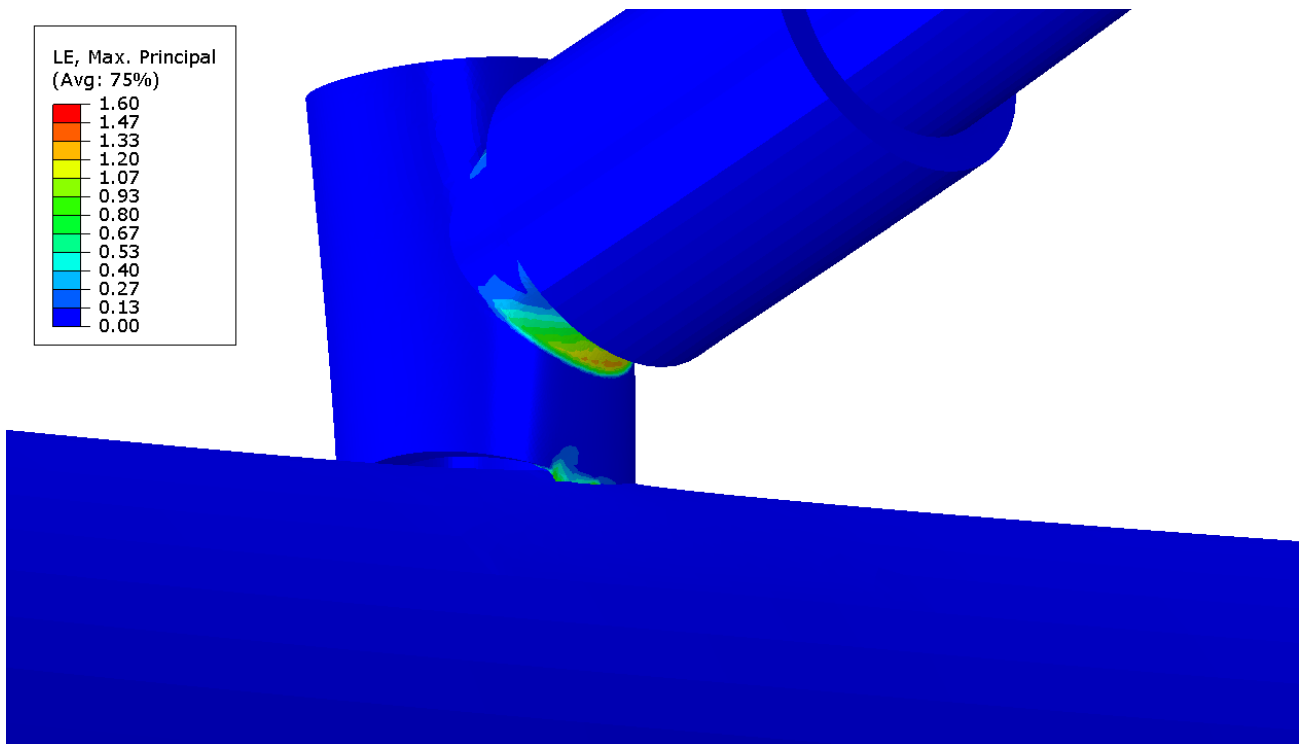


Figure 35. Case 9: Contour plot of maximum principal logarithmic strain.

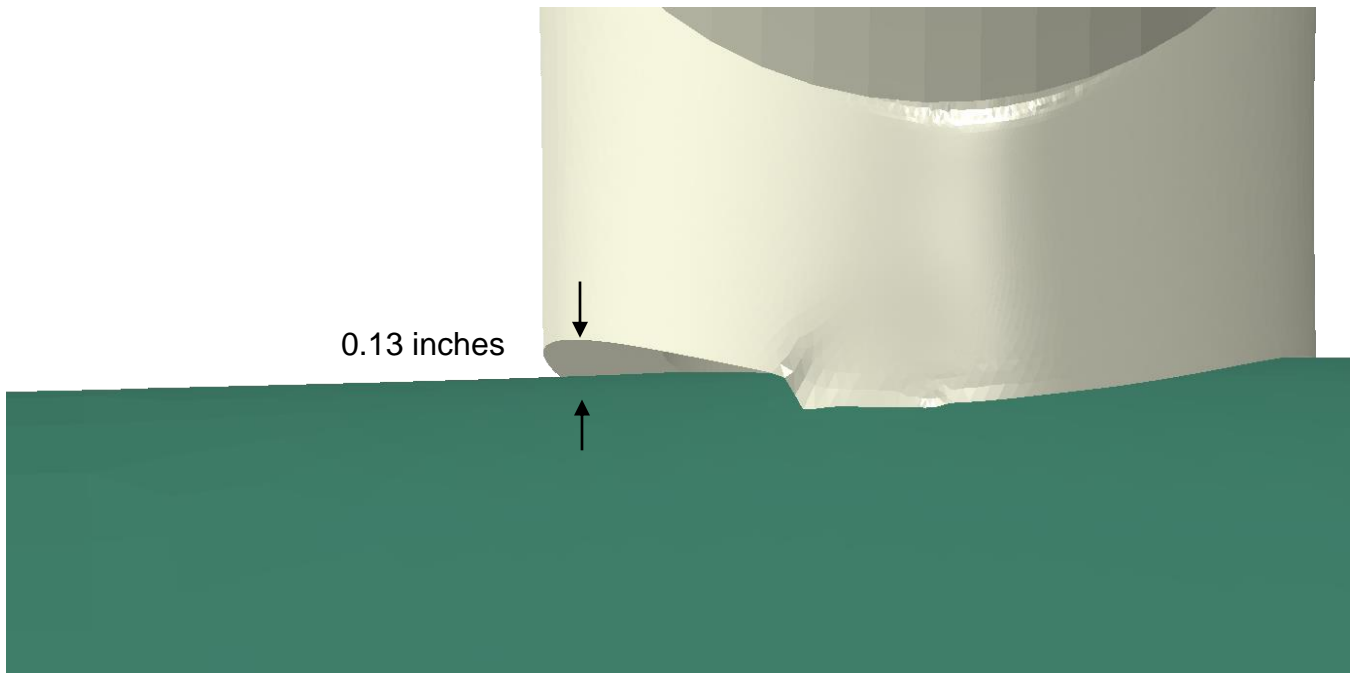


Figure 36. Case 9: Opening at the saddle fusion interface.